Permanent magnet synchronous motor sensorless control based on rotor flux observer with low-pass filter adaptation

D V Bevz, V M Zavyalov
Department of Power Engineering, Tomsk Polytechnic University, Tomsk, Russia
E-mail: d.v.b@mail.ru

Abstract. This paper presents a strategy for a permanent magnet synchronous motor sensorless vector control based on rotor flux estimation considering a rotor saliency. The integration problem in the stator flux estimation was solved by replacing the integrator with a low-pass filter. The low-pass filter parametric adaptation algorithm with phase delay compensation, based on Bode diagrams was designed for the rotor angular position estimation accuracy improving. The proposed adaption algorithm allowed to expand a stable motor control with a high accuracy in the rotor position estimation down to 15 rpm. Also the developed rotor angular position estimation algorithm together with adaptive field weakening algorithm provides a sable motor operation with a high accuracy in the rotor position estimation at the high speed.

1. Introduction

The electric drives based on permanent magnet synchronous motor (PMSM) are in high demand in such industry areas as robotics, tracking and guidance systems, mining, servo systems, medical equipment, electric traction drives, etc. This is explained by that the PMSM has such advantages over another motors type as low values of the electromagnetic and electromechanic time constants, high torque overload capacity, small weight-size parameters compared with other motors type at the same power, wide speed control range, high efficiency (more than 90%). This allows to design high-dynamic electric drives and also makes the PMSM application attractive at the electric drives used in common industry. The PMSM acquired these advantages with new materials emergence for the permanent magnets manufacturing. These materials, as a rule, are Sm-Co, or Ne-Fe-B.

The PMSM control system is based on PMSM mathematical model in the d-q reference frame, fixed relative to the PMSM rotor. The information about rotor position is needed to control PMSM torque and speed. The rotor position is measured by the rotor angular position sensor. However, the rotor position can be calculated by the mathematical expressions describes the PMSM model. It allows to refuse the rotor position sensor using. Failure from the rotor position sensor using allows to reduce PMSM overall dimensions, to increase electric drive reliability, and also to reduce electric drive cost in general. Thus, sensorless control algorithms development is the topic problem to research in the PMSM control algorithms area.

Sensorless control algorithms use the rotor angular position observers based on different mathematical models and using various mathematical methods to estimate the rotor angular position.

PMSM rotor position observers can be divided into two categories: 1) observers using injection of high frequency test signal [1–3]; 2) observers using PMSM mathematical model. The first ones are based on high frequency or pulse signal generation by inverter and the rotor angular position searching by the reaction to this signal. The main disadvantages are additional losses and noise level increasing.

Observers based on PMSM mathematical model, which are called PMSM state observers directly use mathematical expressions of the model to calculate the rotor position [2, 4, 5]. The main disadvantage of these algorithms is the low accuracy of the angular position estimate. In order to improve the accuracy the following methods are used: sliding mode control [6]; Kalman filter [7]; neural networks [8]. The sliding mode control generates a high-frequency component in the estimated rotor angular position, that is required the output signal additional filtering. The algorithms based on Kalman filter or neural networks theory are accompanied by a large amounts of computation, which determines the high requirements for the microprocessor.

Another kind of state observers is observers with adaptive system. The most popular of the adaptive estimation methods is the model reference adaptive system (MRAS) method. This method use PMSM mathematical model equations in order to adapt it to real processes occurring in the motor and, as a result, reduce the orientation error to zero [9]. However, the are no methods for the regulating adapter parameters tuning.

In this paper, the PMSM rotor angular position estimation method that provides stable performances with a high accuracy of rotor position estimation in range from 2 Hz to 400 Hz is considered.

2. State observer for the rotor flux vector angle position estimation

The PMSM rotor angular position will be estimated with PMSM mathematical model in the stationary reference frame α, β.

The PMSM voltage equation in the stationary reference frame is:

$$\begin{bmatrix} v_\alpha \\ v_\beta \end{bmatrix} = \mathrm{R}\begin{bmatrix} i_\alpha \\ i_\beta \end{bmatrix} + \frac{\mathrm{d}}{\mathrm{d}t}\begin{bmatrix} \psi_{s\alpha} \\ \psi_{s\beta} \end{bmatrix}, \tag{1}$$

where:

v_α, v_β – stator voltage in the stationary α, β frame;

i_α, i_β – stator current in the stationary α, β frame;

$\psi_{s\alpha}$, $\psi_{s\beta}$ – stator flux linkage in the stationary α, β frame;

R – stator resistance.

The components of the stator flux linkage are determined by the following expressions:

$$\begin{bmatrix} \psi_{s\alpha} \\ \psi_{s\beta} \end{bmatrix} = \begin{bmatrix} \mathrm{L}_0 + \mathrm{L}_1\cos 2\theta & \mathrm{L}_1 \sin 2\theta \\ \mathrm{L}_1 \sin 2\theta & \mathrm{L}_0 - \mathrm{L}_1\cos 2\theta \end{bmatrix}\begin{bmatrix} i_\alpha \\ i_\beta \end{bmatrix} + \lambda_{\mathrm{PM}}\begin{bmatrix} \cos\theta \\ \sin\theta \end{bmatrix}, \tag{2}$$

where:

λ_{PM} – permanent magnet flux linkage;

θ – rotor position;

$$\mathrm{L}_0 = \frac{\mathrm{L_d} + \mathrm{L_q}}{2},\ \mathrm{L}_1 = \frac{\mathrm{L_d} - \mathrm{L_q}}{2},$$

L_d and L_q are the d- and q-axes inductances.

As the initial equations for estimating θ, we take the equations system (2). Express from them the components with angle θ and permanent magnet flux linkage λ_{PM}:

$$\lambda_{\mathrm{PM}}\begin{bmatrix} \cos\theta \\ \sin\theta \end{bmatrix} = \begin{bmatrix} \psi_{s\alpha} \\ \psi_{s\beta} \end{bmatrix} - \begin{bmatrix} \mathrm{L}_0 + \mathrm{L}_1\cos 2\theta & \mathrm{L}_1 \sin 2\theta \\ \mathrm{L}_1 \sin 2\theta & \mathrm{L}_0 - \mathrm{L}_1\cos 2\theta \end{bmatrix}\begin{bmatrix} i_\alpha \\ i_\beta \end{bmatrix} \tag{3}$$

Then:

$$\frac{\sin\theta}{\cos\theta} = \tan\theta = \frac{\psi_{s\beta} - \left(\mathrm{L}_0 - \mathrm{L}_1\cos 2\theta\right) i_\beta + \mathrm{L}_1 \sin 2\theta i_\alpha}{\psi_{s\alpha} - \left(\mathrm{L}_0 + \mathrm{L}_1\cos 2\theta\right) i_\alpha + \mathrm{L}_1 \sin 2\theta i_\beta} \tag{4}$$

Thus, the rotor angular position is:

$$\theta = \arctan\left[\frac{\psi_{s\beta} - \left(L_0 - L_1 \cos 2\theta\right) i_\beta + L_1 \sin 2\theta i_\alpha}{\psi_{s\alpha} - \left(L_0 + L_1 \cos 2\theta\right) i_\alpha + L_1 \sin 2\theta i_\beta}\right] \tag{5}$$

The values $\psi_{s\alpha}$ and $\psi_{s\beta}$ can be determined by integration of (1):

$$\begin{cases} \psi_{s\alpha} = \int_o^t \left(v_\alpha - R i_\alpha\right) dt; \\ \psi_{s\beta} = \int_o^t \left(v_\beta - R i_\beta\right) dt. \end{cases} \tag{6}$$

Integration in (6) accumulates error if there is constant component. In order to eliminate this drawback the integrators are replaced by 1st order low-pass filters with the following transfer function:

$$W(s) = \frac{T}{Ts + 1}, \tag{7}$$

where T is low-pass filter cutoff frequency.

It is recommended to choose the cutoff frequency in the range 1 – 3 Hz [10]. Figure 1 shows Bode plots of the integrator and low-pass filter with cutoff frequency 3 Hz. Low-pass filter gain and phase shift will be identical to the integrator at the nominal motor speed ω_{nom}. The phase error will be increase up to 45° with a decrease in speed from ω_{nom} to ω_c. This will lead to stator flux linkage estimation error increasing.

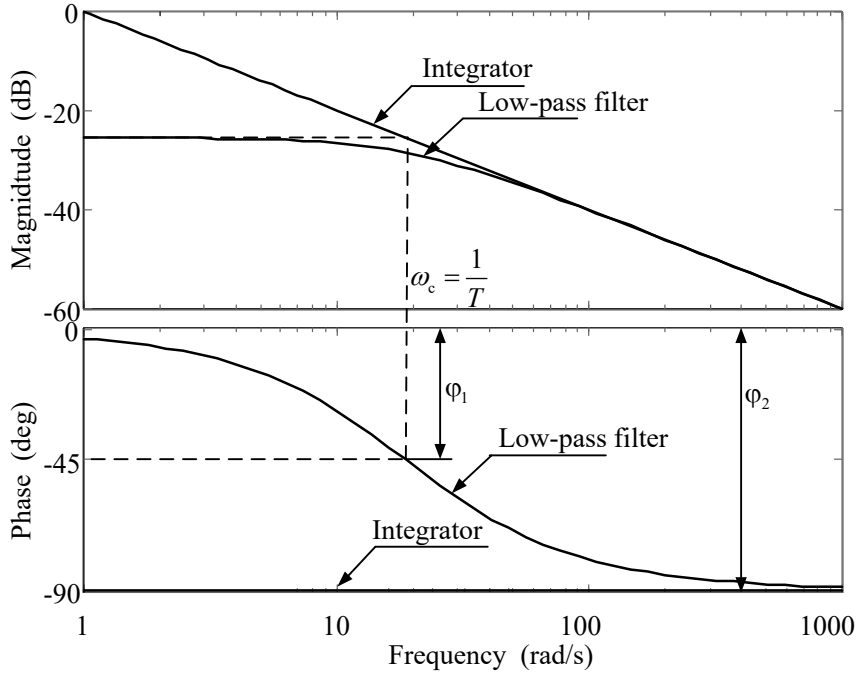

Figure 1. The low-pass filer and integrator Bode plots.

Figures 2 and 3 show that the phase error in ψ_s estimation have the greatest influence on the accuracy of the λ_{PM} angular position estimation, which determines the rotor angular position.

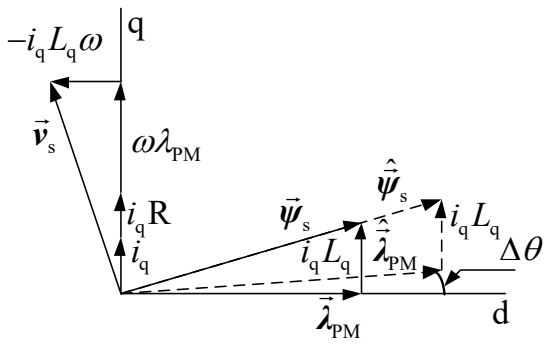

Figure 2. Error in stator flux linkage vector amplitude estimation on PMSM vector diagram.

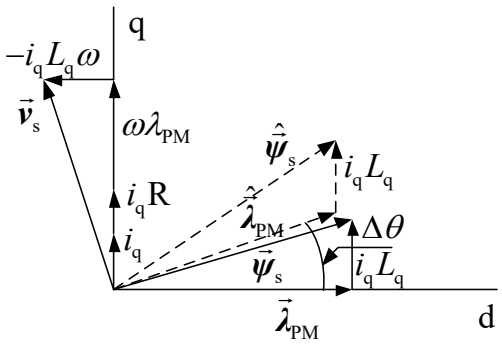

Figure 3. Error in a stator flux linkage vector angular position estimation on PMSM vector diagram.

3. Proposed low-pass filter adaptation algorithm developing

We will use low-pass filter time constant adaptive tuning depending on the motor shaft rotation frequency to ensure a constant phase shift of -45°. The adaptive tuning is to set the low-pass filter cutoff frequency equals to the current electrical rotation frequency. Thus, the time constant $T = f(\omega_{el})$. The low-pass filter Bode plots with adaptive tuning are shown in Figure 4.

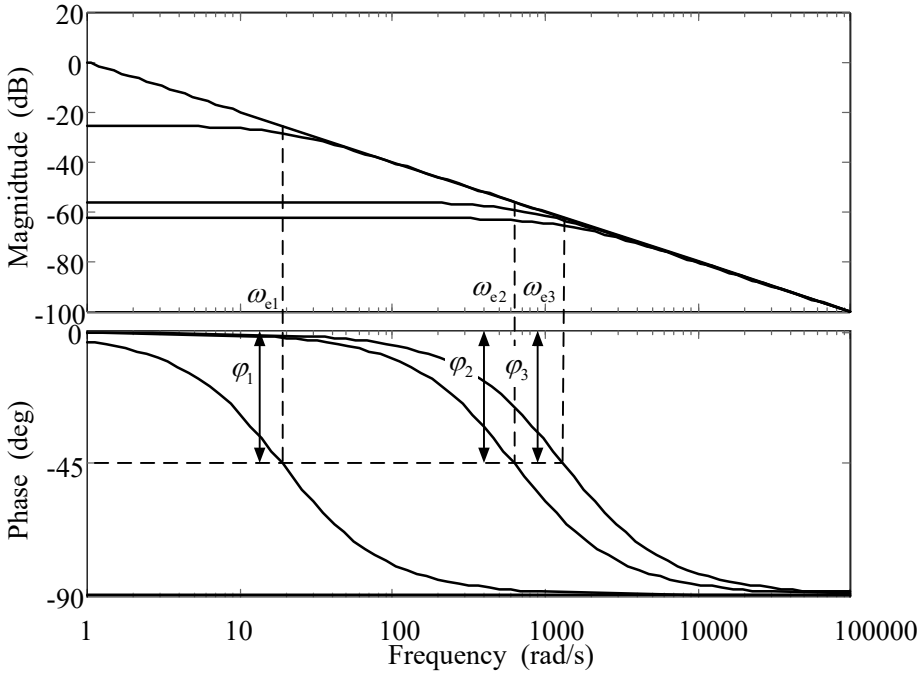

Figure 4. The low-pass filter Bode plots with proposed adaptation algorithm.

Then, to obtain a phase shift of -90° it is necessary to provide an additional phase shift of -45°at filter output. As a result, the low-pass filter using with angle correction to determine the stator flux linkage will provide a phase shift identical to the integrator, without error accumulation at the motor low speed operation. This will make it possible to obtain accurate rotor position estimation at the low speed.

4. Experimental results

The rotor angular position observer algorithm was developed for the fan electric drives based on PMSM sensorless control. Also, a frequency converter EC-F with a rated power of 3 kW and three-phase AC voltage of 380 V was designed to control a PMSM. PMSM parameters are presented in table 1.

Table 1. Parameters of the PMSM.

Number of poles pairs (p)	8
Rated power	2.2 kW
Rated speed	1500 rpm
Rated frequency	200 Hz
Rated torque	14 Nm
Rated phase to phase voltage	380 (rms)
Rated pahse current	4.2 A(rms)
Stator resistance per phase (R_s)	2.4 Ω
d-axis inductance (L_d)	101 mH
q-axis inductance (L_q)	133 mH
Rotor permanent – magnet (λ_{PM})	0.213 V s rad-1

The frequency converter EC-F is based on digital signal processor STM32F405G. The sampling frequency is set to 5 kHz and the PWM frequency is set to 20 kHz. The dead time of IGBT inverter is set to 1 μs. The experimental setup with a radial fan is shown in Figure 5.

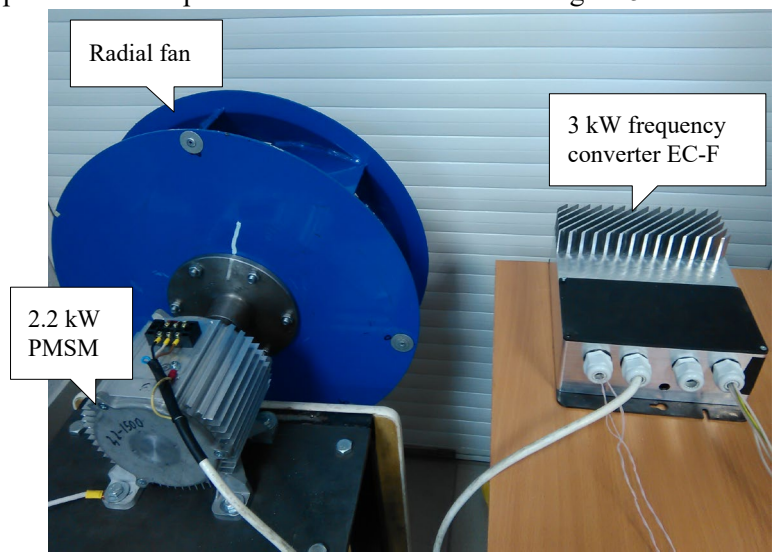

Figure 5. Experimental setup with a radial fan.

PMSM sensorless control is based on vector filed-oriented control, where the rotor angular position and the rotation speed are estimated by the observer. In parallel, the actual rotor angular position was measured by incremental encoder with 2500 pulses per revolution.

The electric drive start-up begins with initial rotor angular position identification. The identification is carried out when a stator current is formed along the d-axis and zero angle applied to Park transformations. During this this time the observer estimates the rotor angular position. Then the control structure switches to current control along the q-axis and current vector rotates on angle, which is estimated by observer.

The estimated rotor position $\hat{\theta}$ and the actual rotor position θ are shown in Figures 6–8, where 1 relative unit equals 360 electrical degrees.

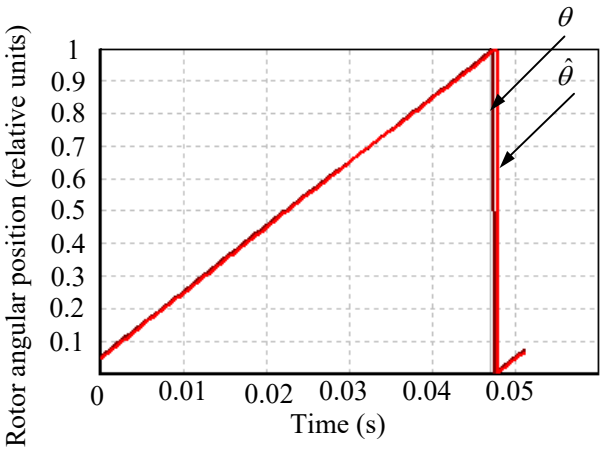

Figure 6. Rotor angular position at the rotation speed of 20 rpm.

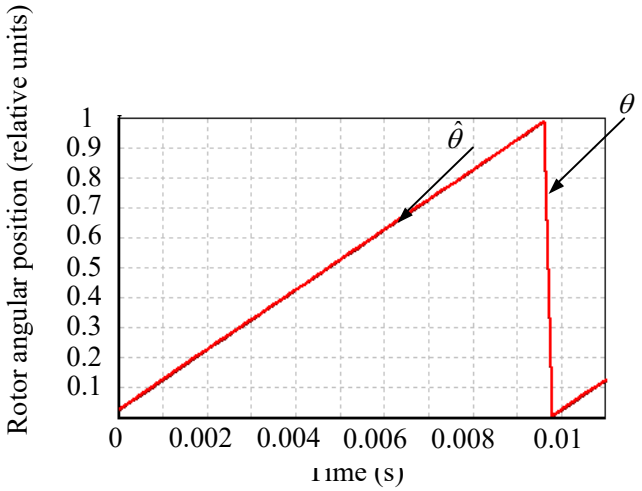

Figure 7. Rotor angular position at the rotation speed of 750 rpm.

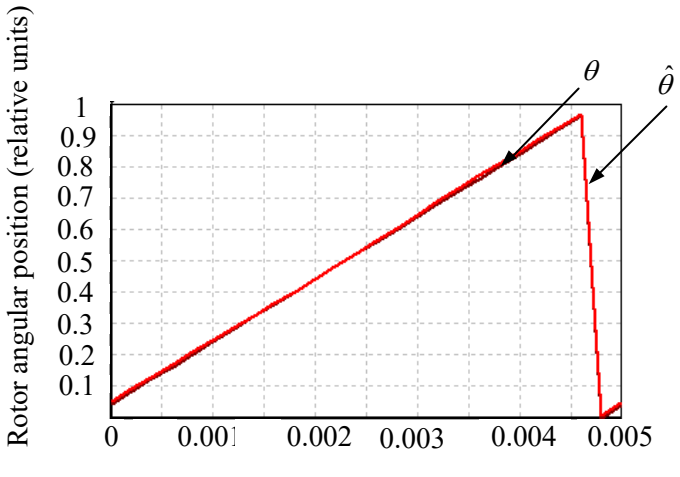

Figure 8. Rotor angular position at the rotation speed of 1500 rpm.

The information about error between estimated and actual angle rotor position is presented in table 2.

Table 2. The observer characteristic.

Speed reference ω, p.u.	The rotor position estimation error $\Delta\theta$,°	
	f_c = 3 Hz	$f_c = \frac{\omega_{el}}{2\pi}$
0.01	3.915	0.423
0.1	2.85	0.423
0.5	1.89	0.325
1.0	1.525	0.426
2.0	1.635	0.485

Transient performances at the electric drive accelerate are shown on Figures 9 and 10, where 1 relative unit for speed equals 1500 rpm and 1 relative unti for current equals 5 A.

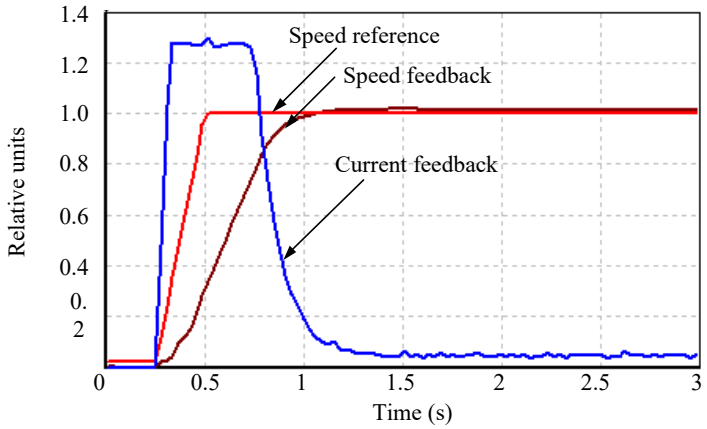

Figure 9. Electric drive speed and torque transient performances at speed reference of 1500 rpm.

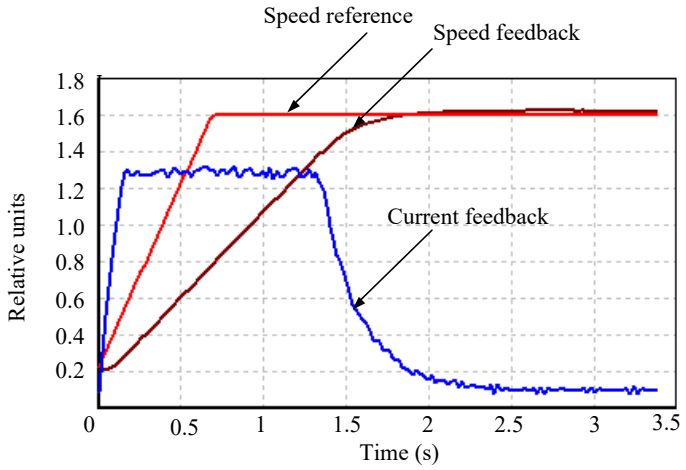

Figure 10. Electric drive speed and torque transient performances at speed reference 2400 rpm.

In order to expand speed control range, field weaking algorigm “Constant current – constant power” (CCCP) was applied.

Figure 11 shows experimental setup for proposed observer algoritm research with a different load on the PMSM shaft. The inducton motor of rated power 5.5 kW with control from Danfoss FC302 are used to provide a load.

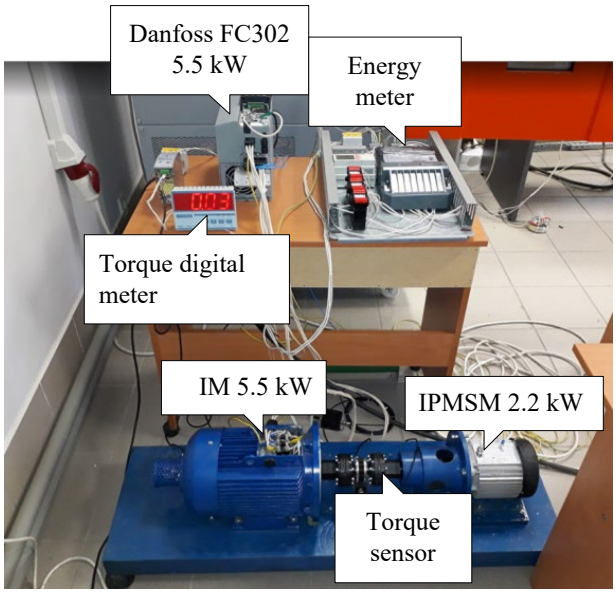

Figure 11. Experimental setup with a load machine.

The limiting electromechanical characteristic of PMSM when it is opertaed in sensorless mode is shown in Figure 12. Sensorless control provides a stable operation at the dobule electromechanical torque overload in speed range from 250 rpm to 1150 rpm.

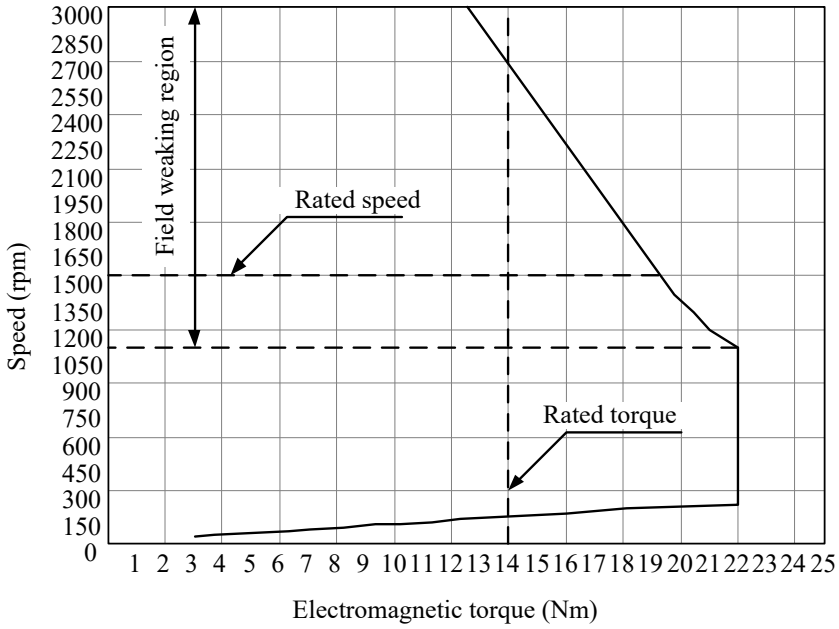

Figure 12. PMSM electromechanical characteristic with vector control based on rotor position observer.

5. Conclusion

The developed rotor angular position estimation method provides a stable motor control in closed speed loop at the speed range from 15 rpm to 3000 rpm. The error between actual rotor position and estimated rotor position no more 1 mechanical degree The low-pass filter time constant adaptive tuning is showed significant error decreasing in the rotor angular position estimation, especially at low speed operation. The observer algorithm provides a low computing load on the processor and can be integrated into any electric drive control system.

However, there is no ability to reverse. Also, the maximum electromagnetic torque is decreased with a speed decreasing form 150 rpm to 15 rpm. Analysis and improvement of the observer dynamic performances, expansion the load range at the low speed operation and the ability to revers are directions for further research.

References

[1] Briz F, Diez A and Degner M W 2000 *IEEE Transaction on Industry Applications* **36** pp 1360–68
[2] Sul S, Kwon Y and Lee Y 2017 *Ces Transactions on Electrical Machines and Systems* **1** pp 91–99
[3] El-Murr G, Giaouris D and Finch J W 2009 *Proceedings of the 2008 IEEE Reagion 10 and the Third international Conference on Industrial and Information Systems* pp 1–6
[4] Bedetti N, Calligaro S and Petrella R 2013 *IEEE Energy Conversion Congress and Exposition* pp 3496–3503
[5] Inoue T, Hamabe Y, Tsuji M and Hamasaki S 2018 *The 2018 Internattional Power Electronics Conference* pp 1276–81
[6] Lee H and Lee J 2013 *IEEE Transactions On Control Systems Technology* **21** pp 1394–99
[7] Termizi M S, Lazi J M, Ibrahim Z, Talib M H N, Aziz M J A and Ayob S M 2018 *IEEE Conference on Energy Conversion* pp 145–150
[8] Ren Y and Zhou L 2018 *Cyberworlds 2008 International Conference* pp 1823–29
[9] Kumar P, Kumar M and Dahiya S 2015 *Proceedings of the World Congress on Engineering* pp 198–204
[10] Holtz J 2002 *IEEE Electrical Machines and Drives Group* **90** pp 1359–94